Multi-wavelength, multi-angular lidar for aerosol characterization

Andrea M. Wyant*[a], David M. Brown[a], Perry S. Edwards[a], and C. Russell Philbrick[a,b,c]
[a]Dept. of Electrical Engineering, Penn State University, University Park, PA, USA 16802;
[b]Dept. of Physics, and [c]Dept. of Marine, Earth, and Atmospheric Sciences,
North Carolina State University, Raleigh, NC USA 27606

ABSTRACT

A multi-wavelength, multi-static lidar has been designed and is being tested for the characterization of atmospheric aerosols. This design builds upon multi-static lidar, multiple scattering analyses, and supercontinuum DIAL experiments that have previously been developed at Penn State University. Scattering measurements at two polarizations are recorded over a range of angles using CCD imagers. Measurements are made using three discrete visible wavelength lasers as the lidar sources, or using a supercontinuum source with a wavelength range spanning the visible and near-IR wavelengths. The polarization ratios of the scattering phase functions are calculated for multiple wavelengths to analyze and determine the aerosol properties of artificially generated fog.

Keywords: aerosol characterization, aerosol size distribution, multi-static lidar, multi-wavelength lidar, polarization ratio, scattering phase function

1. INTRODUCTION

Aerosol characterization has become an increasingly important area of research in response to growing environmental and defense concerns. With the capability of remotely determining size distributions, number densities, refractive indices, and particle shape, much can be learned about the role of aerosols in our atmosphere. The scattering phase function of a volume of particles contains a wealth of information relating to the shape and size distribution of the aerosol content. It has been demonstrated by several research groups[1-5] that it is possible to retrieve size distribution profiles remotely by examining the scattering phase function from a range of angles. The selected observation angles, the resolution of these angles, and excitation wavelength choice are important when attempting to perform this characterization. Studies that invoke the use of three CCD imagers[2, 3] have demonstrated aerosol characterization performance when using a single excitation wavelength, when the atmosphere is fairly uniform across the field-of-view of the imager. However, when sharp layers occur in the aerosol features as a function of altitude it became impossible to invert aerosol size distribution from the scattering phase functions. It was suggested that adding multiple wavelengths to the analysis would constrain the inversion for an accurate retrieval of aerosol size distributions, concentrations, and refractive index even under conditions of a non-uniformly mixed atmosphere. A supercontinuum laser source, or white light laser, would provide a spectrum of excitation wavelengths simultaneously, while a CCD imager equipped with the appropriate grating could retrieve and interpret the scattered phase function in high spatial and spectral resolution. This multi-dimensional dataset could then be used to retrieve the shape and size distribution of an aerosol scattering volume with a high level of accuracy. The described measurement approach features highly portable hardware and is robust enough to provide accurate measurements in both a laboratory chamber measurement or a field test without any system modifications.

2. THEORY

The scattering of light from a collection of particles is dependent on many properties of both the particles and the incident light. The wavelength and polarization of the incident light determine the scattering, along with the refractive index, the number density, the size distribution, and the shape of the particles.

*amw351@psu.edu

Laser Radar Technology and Applications XIV, edited by Monte D. Turner, Gary W. Kamerman,
Proc. of SPIE Vol. 7323, 73230R · © 2009 SPIE · CCC code: 0277-786X/09/$18 · doi: 10.1117/12.818686

The large number of variables makes it impossible to remotely characterize unknown aerosols using only backscattering measurements at a single wavelength. Additional information can be gathered by examining not only the light scattered directly back, but also the light scattered at other angles by the aerosols. Fig. 1 shows how the scattering phase function changes for perpendicular polarized light, i_1, and parallel polarized light, i_2, as the parameter *ka* increases. The quantity *ka* relates the propagation number ($k = 2\pi/\lambda$) to the radius of the aerosol, *a*.

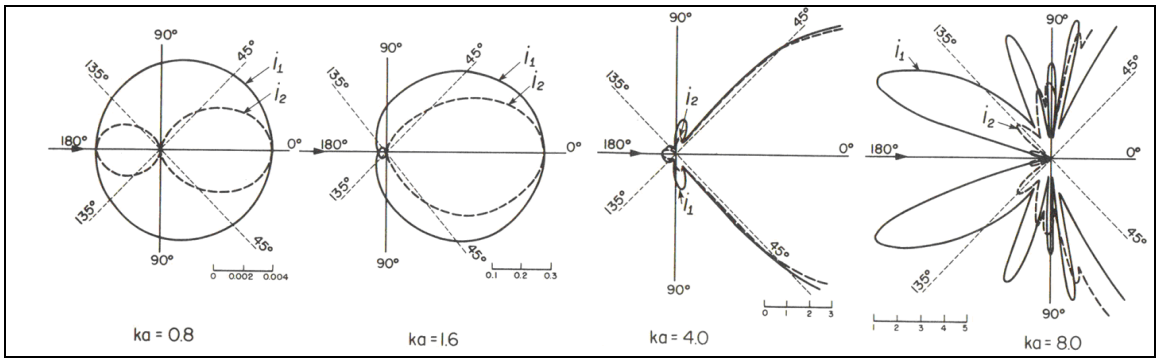

Fig. 1: Scattering of polarized light as a function of angle and particle radius.[6]

The geometry of the multi-static system, shown in Fig. 2, is such that the length of the aerosol volume imaged by each pixel is proportional to the squared distance from the imager to the volume. This proportionality approximately cancels the R^2 dependence that is traditionally in the lidar equation, and allows imagers with a smaller dynamic range to be used in the system.[1, 7]

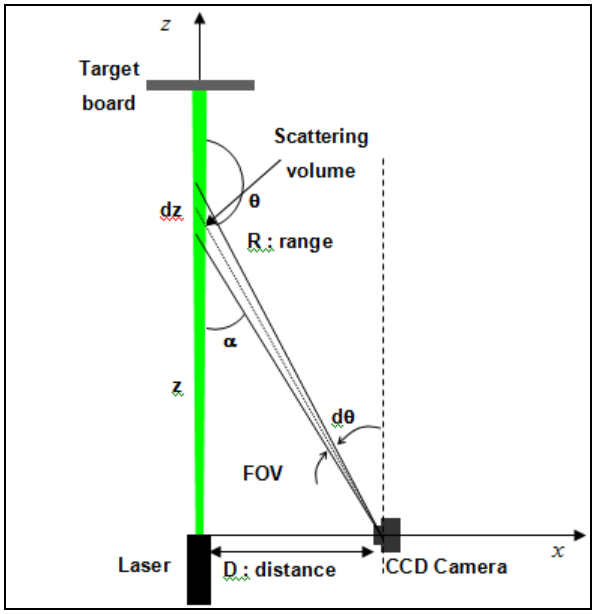

Fig. 2: Multi-static lidar geometry[8]

The polarization ratio, which will be used as the principle data for the aerosol characterization, is formed by dividing the parallel polarized scattering intensity by the perpendicular polarized scattering intensity. Forming a pixel-by-pixel ratio of the imaged parallel and perpendicular phase functions eliminates a lot of complexity from the remote sensing lidar equation. In particular, the path extinction from the scattering volume to the imager is cancelled from this analysis. The power of the received signal by the multi-static system can be calculated as,

$$P_r = P_t \frac{C}{D} \beta(z,\theta) T^2 d\theta \tag{1}$$

where C is dependent on the system parameters, D is the linear distance from the detector to the imaged aerosol volume, β is the scattering coefficient, and T^2 is the two-way atmospheric transmittance.[8] When the system design is such that only the backscattering coefficients contain polarization dependence, then the equation for the polarization ratio reduces to

$$\delta_p = \frac{P_{r,\parallel}}{P_{r,\perp}} = \frac{P_t \frac{C}{D} \beta_\parallel(z,\theta) T^2 d\theta}{P_t \frac{C}{D} \beta_\perp(z,\theta) T^2 d\theta} = \frac{\beta_\parallel(z,\theta)}{\beta_\perp(z,\theta)} \tag{2}$$

System parameters, such as the spectral response of the transmitter optics and the detector, and nonlinearities across the field-of-view of the detector, and path extinction between the scattering volume and the detector, do not introduce added complexity when the polarization ratio is analyzed.

3. EXPERIMENTAL SET-UP

Three lasers at wavelengths of 407nm, 532 nm, and 650 nm are co-aligned into a single transmitted beam. Co-alignment of the three lasers for the tri-laser experiment is important, as the scattering from each beam must be in the same horizontal plane imaged by the CCD camera. This co-aligned setup ensures that the sampled volume is equivalent for each laser wavelength, as opposed to having the transmitted beams spatially separated. Mapping the scattering phase function along the axis of the beam requires that the particle size distributions are uniform along the imaged path. Previous investigations, in addition to initial experiments of this work, have shown that the size distribution of aerosols is largely constant on any given horizontal plane. After co-alignment, the beam is sent through a polarizing beamsplitter, which transmits only the polarization component that is parallel to the scattering plane. A half-waveplate, mounted on a flip-mirror, can be placed into the beam to rotate the polarization by 90 degrees. Another flip-mount mirror is used to fold the supercontinuum into the transmit path, thereby blocking the three discrete wavelength lasers. The power spectrum of the supercontinuum source is shown in Fig. 3. The experimental transmitter setup is depicted in Fig. 4. A transmission diffraction grating is used to vertically spread the three wavelengths on the CCD imager, as shown in Fig. 5, which allows separate analysis at each wavelength. The camera is a Meade Deepsky Pro II with a 48° field-of-view focusing lens.

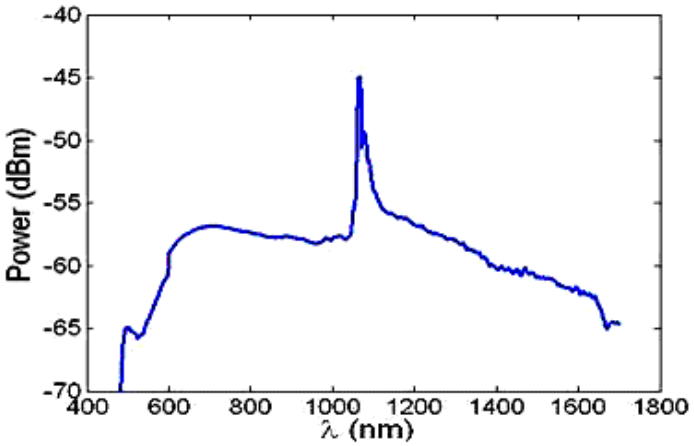

Fig. 3: Power spectrum of supercontinuum source

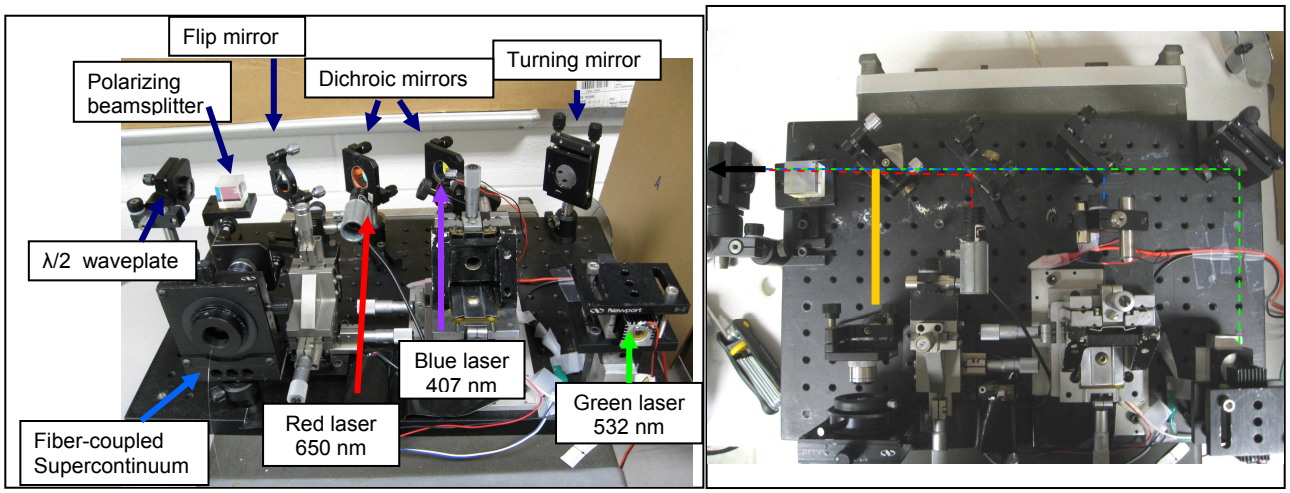

Fig. 4: Picture of the transmitter setup (a) from the side and (b) from the top

Fig. 5: Picture of Meade Deepsky Pro II imager and transmission diffraction grating setup

The artificially generated polyalpha olefin (PAO) smoke is held by an aerosol chamber (122 cm long, 122 cm wide, and 21 cm high) located approximately two meters distant from the transmitter. A viewing window is located on the entrance-side of the chamber to measure scattering angles of approximately 122 through 170 degrees, as shown in Fig. 6.

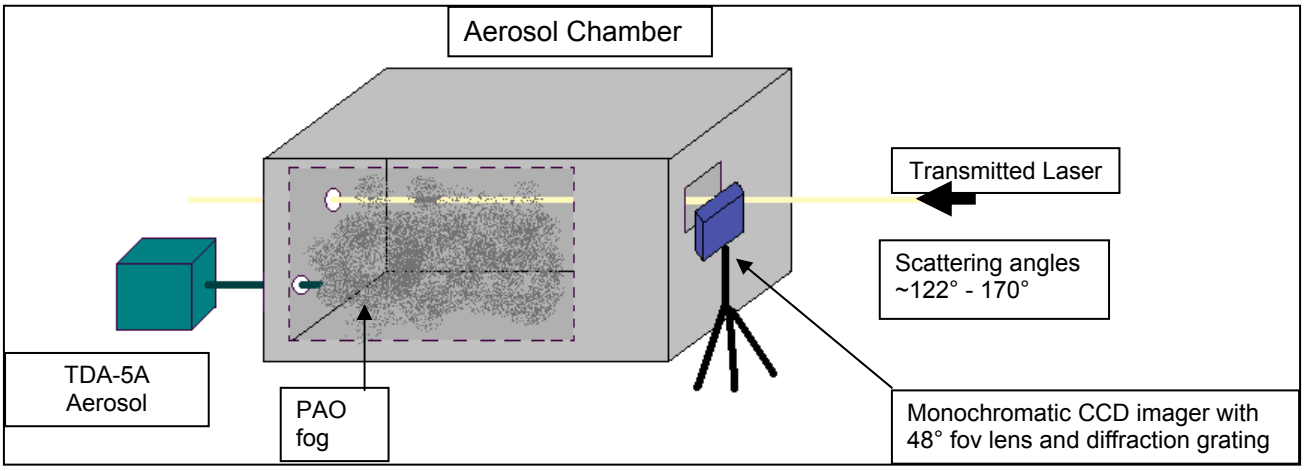

Fig. 6: PAO aerosol experimental setup

An image of the 1st order diffracted parallel polarized scattering intensity is taken as the beam transverses the aerosol chamber. A half-waveplate is placed into the beam in order to rotate the polarization from parallel to perpendicular and a second image is taken. An example of such an image is shown in Fig. 7.

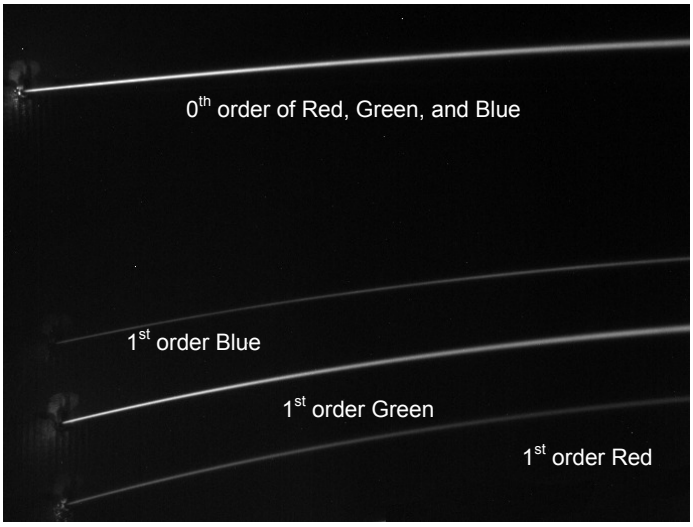

Fig. 7: Image of combined discrete lasers through the diffraction grating

3.1 Data processing

The first task of data analysis is accurately extracting the scattering intensity data from the CCD image. Although it is difficult to perceive from the raw data of the beams separated with the grating, variation in the scattering phase function can be extracted through a series of processing techniques. Examination of Fig. 7 will reveal a slight bend to each of the 'rows' of scattering intensities. This bend is caused by optical scattering from the diffraction grating and adds some complexity to the analysis of the image. An alignment image was used to accurately extract the spatial location and assign an angle to the intensities from the image. Vertical strings were equally spaced along the length of the box and an image is taken of the lasers striking the strings. A thresholding and a center-finding algorithm are used on the alignment image in order to locate the pixel in the center of each of the bright spots produced by the laser striking the strings. A second order polynomial fit to the center pixels of each 'row' are used to extract the scattering data for each wavelength from the scattering images. The beam profile is examined for each diffracted laser as a function of column. The 25% intensity point on each side of the maximum intensity point is used to determine the number of rows to integrate across for each diffracted laser beam. The steps in the data extraction technique are illustrated in Fig. 8 and Fig. 9.

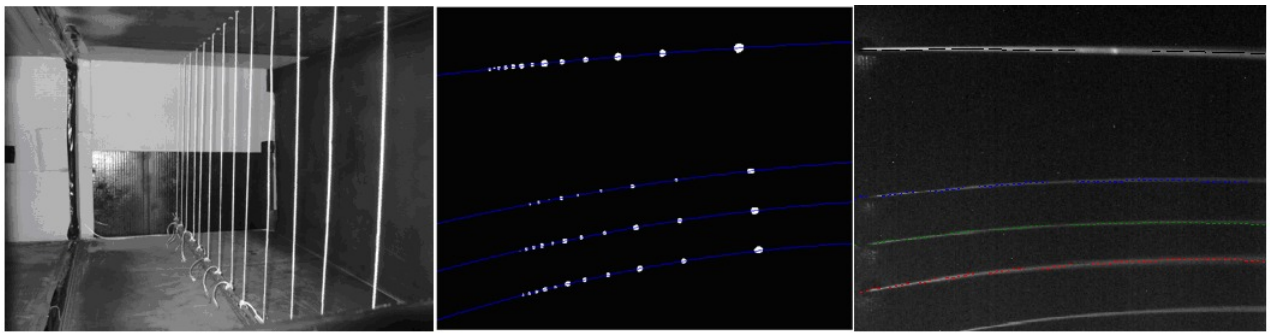

Fig. 8: Method for data extraction

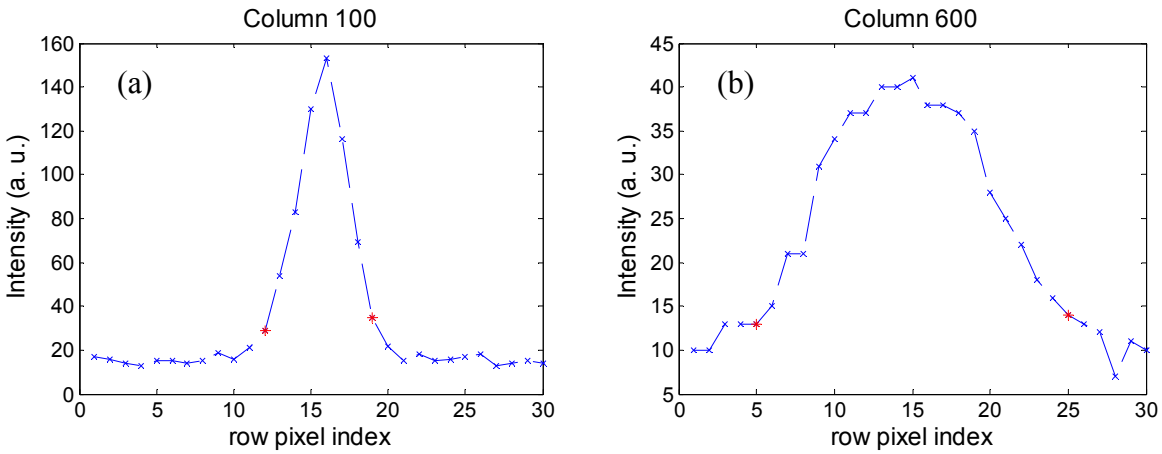

Fig. 9: Beam profile of diffracted 532 nm laser at (a) left side of image (column 100) and at (b) right side of image (column 600)

4. RESULTS AND COMPARISONS

Scattering images of both perpendicular and parallel polarizations were taken using the tri-laser transmitter and the supercontinuum transmitter. The average size distribution of the PAO fog produced by the TDA-5A aerosol generator was measured 30 times by Park[8] and a lognormal distribution was fit to the averaged data to find a geometric mean diameter of 230 nm and a geometric standard deviation of 1.66 (Fig.10). A Mie code program, MIETAB[9], is used to calculate the expected polarization ratios of the artificially generated fog based on these previous scanning mobility particle sizer (SMPS) measurements. Experimental polarization ratios obtained using the three discrete lasers match favorably with the theoretical calculated ratios as shown by Fig. 11. The differences are most likely due to the generated fog having a slightly different size distribution than the averaged lognormal distribution used in the theoretical calculations. Additional experiments will be performed to reproduce the tri-laser results in an initial dataset to refine the data extraction and inversion approaches. Each particle size distribution will have a range of angles and wavelengths that are optimal for data inversion, ultimately leading to the remote characterization of particle size and shape distribution.

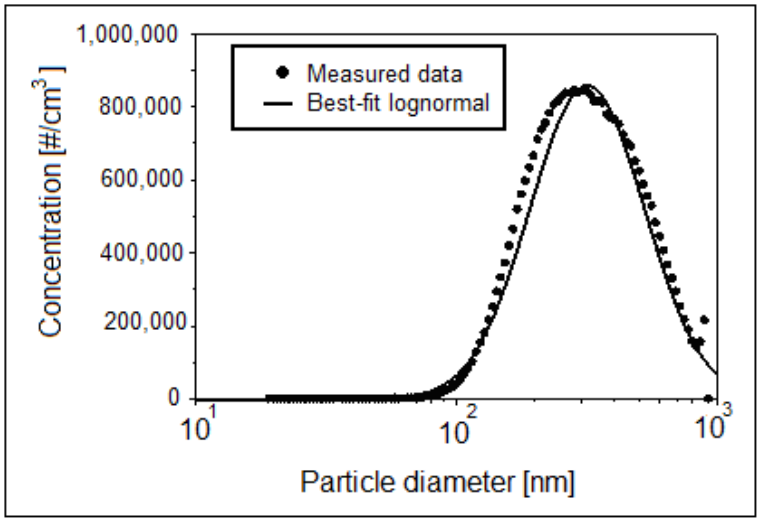

Fig. 10: Particle size distribution measured by scanning mobility particle sizer.[8]

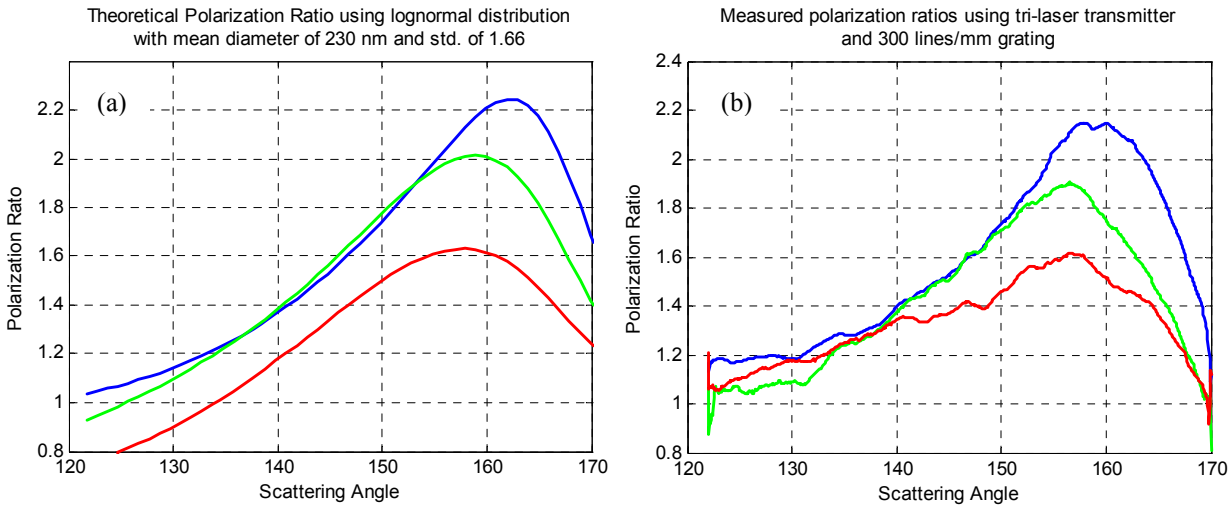

Fig. 11: Comparison of (a) calculated polarization ratio using MIETAB[9] and (b) measured polarization ratio using combined 407 nm, 532 nm, and 650 nm discrete laser transmitter.

Initial supercontinuum aersosol scattering measurements were completed using the constructed aerosol chamber and a 10 mW supercontinuum source. Fig. 12 shows the results of the initial parallel (left) and perpendicular (right) scattering measurements. The tri-laser images were used to determine the wavelength span of the supercontinuum measurement. Through this calibration, it was found that most of the power in the continuum spectrum is in the infrared region, outside of the operational range of the optics integrated into this transceiver. Although the half waveplate was not optimized for the infrared region, variation in the scattering angle can be noted in each figure shown, roughly corresponding to orthogonal polarizations of excitation. A 600 ln/mm grating was used to make an alternate scattering measurement offering more wavelengths for the inversion step of the analysis. By using the high resolution grating and spreading the light more extensively across the CCD chip the number of photons per pixel is reduced, and the measurement is closer to the noise floor of the detector. Until the power of the supercontinuum source can be increased, the experiment requires the low resolution grating, which increases the power density per pixel at the cost of spectral resolution.

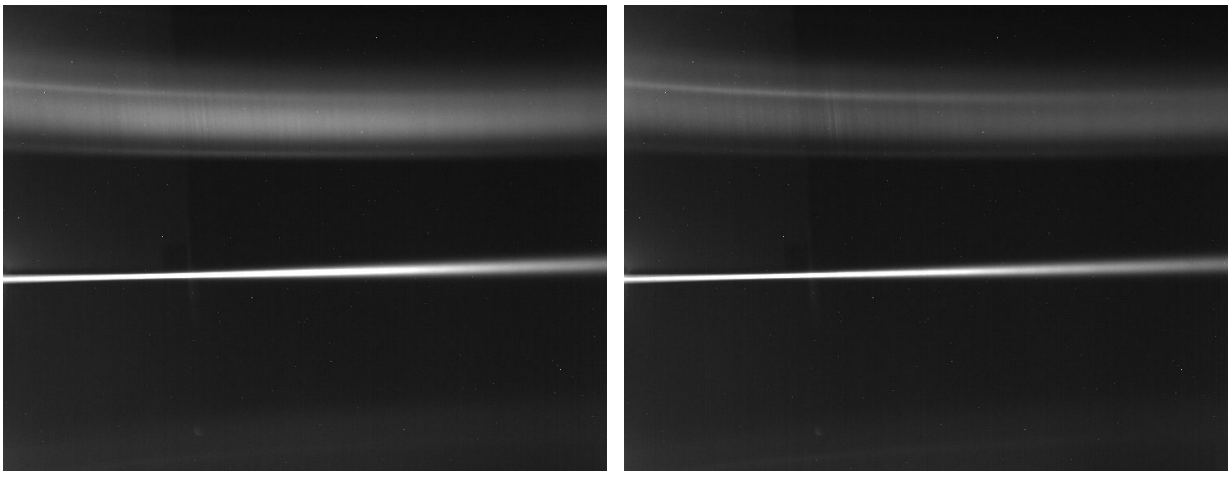

Fig. 12: CCD image through 300 lines/cm diffraction grating (a) supercontinuum parallel polarization (b) supercontinuum perpendicular polarization

5. CONCLUSION

The multi-wavelength, multi-angular approach to characterization of aerosols may have some advantage over classical aerosol characterization techniques, such as aerodynamic particle size (APS) units, because the scattering properties of aerosols of interest are measured directly. In contrast, aerodynamic sizing units rely on the assumption that the particles examined are spherical, which then leads to a size bin classification based on their aerodynamic flow field properties. The added information gained by extending the multi-static approach to multiple wavelengths, leads to a more constrained, and thus, a more accurate inversion for aerosol size distributions, concentrations, and refractive indices. After further refinement, supercontinuum aerosol scattering may be able to remotely characterize the shape distribution of aerosolized targets of interest by oversampling the aerosol volume through a multitude of wavelength and angular measurements. Initial scattering measurements using collinear visible wavelengths and a controlled aerosol release demonstrate the feasibility of the approach to remotely characterize the size distribution of aerosols within a laboratory chamber. Future laboratory and field measurements will be used to show the validity of the technique under a variety of atmospheric conditions.

REFERENCES

[1] Stevens, T. D., "Bistatic Lidar Measurements of Lower Tropospheric Aerosols", Ph. D Thesis, Pennsylvania State University, (1996).

[2] Novitsky, E. J., "Multistatic Lidar Profile Measurement of Lower Troposphere Aerosol and Particulate", Ph. D Thesis, Pennsylvania State University, (2002).

[3] Novitsyky, E. J. and Philbrick, C. R., "Multistatic Lidar Profiling of Urban Atmospheric Aerosols," JGR Atmosphere, 110, D07S11+ (2005).

[4] Barnes, J. E., Bronner, S., Beck, R., and Parikh, N. C., "Boundary layer scattering measurements with a charge-coupled device camera lidar," Applied Optics, 42(15), 2647-2652 (2003).

[5] Olofson, K. F. G., Witt, G., and Pettersson, J. B. C., "Bistatic lidar measurements of clouds in the Nordic Arctic region," Applied Optics, 47(26), 4777-4786 (2008).

[6] Born, M. and Wolf, E., [Principles of Optics: Electromagnetic Theory of Propagation, Interference and Diffraction of Light (7^{th} edition)], Cambridge University Press, Cambridge, United Kingdom, (1999).

[7] Meki, K. Yamaguchi, K., Li, X., Saito, Y., Kawahara, T. D., and Nomura, A., "Range-resolved bistatic imaging lidar for measurement of the lower atmosphere," Optics Letters, 21(17), 1318-1320 (1996).

[8] Park, J. H., "Multiple Scattering Measurements using Multistatic Lidar", Ph. D Thesis, The Pennsylvania State University, (2008).

[9] Miller, A., "MieTab: A scattering program for Windows," [online] 2008, http://amiller.nmsu.edu/mietab.html (Accessed: 1 August 2008).